

RSC Advances



This is an *Accepted Manuscript*, which has been through the Royal Society of Chemistry peer review process and has been accepted for publication.

Accepted Manuscripts are published online shortly after acceptance, before technical editing, formatting and proof reading. Using this free service, authors can make their results available to the community, in citable form, before we publish the edited article. This *Accepted Manuscript* will be replaced by the edited, formatted and paginated article as soon as this is available.

You can find more information about *Accepted Manuscripts* in the [Information for Authors](#).

Please note that technical editing may introduce minor changes to the text and/or graphics, which may alter content. The journal's standard [Terms & Conditions](#) and the [Ethical guidelines](#) still apply. In no event shall the Royal Society of Chemistry be held responsible for any errors or omissions in this *Accepted Manuscript* or any consequences arising from the use of any information it contains.

1 An Integrated Metabonomics and Microbiology
2 Analyses of Host-Microbiota Metabolic Interactions
3 in Rats with *Coptis chinensis*-Induced Diarrhea

4 Yemeng Li,^{#a} Qiongfeng Liao,^{#b} Manna Lin,^{ab} Danmin Zhong,^a Lin Wei,^a Bo Han,^c Hui Miao,^a
5 Meicun Yao,^a and Zhiyong Xie ^{*a}

6 ^aSchool of Pharmaceutical Sciences, Sun Yat-sen University, Guangzhou, 510006, P. R. China

7 ^bSchool of Chinese Materia Medica, Guangzhou University of Chinese Medicine, Guangzhou, 510006, P. R. China

8 ^c School of pharmacy, Shihezi University, Shihezi, 832000, P. R. China

9 *Corresponding author: Zhiyong Xie

10 Tel: +86 20 39943047

11 Fax: +86 20 39943000

12 E-mail address: xiezy2074@yahoo.com

13 [#]These authors contributed equally to this work.

14

15 Abstract

16 *Coptis chinensis* Franch., a berberine-containing traditional Chinese medicine (TCM), is often
17 used to treat intestinal infections, diabetes and hyperlipidaemia, and often causes diarrhea. To
18 clarify the potential mechanism of toxicity that induces diarrhea, Sprague-Dawley (SD) rats were
19 treated with *Coptis chinensis* dosage of 5 g/kg for 14 consecutive days. PCR-denaturing gradient
20 gel electrophoresis (PCR-DGGE) was used to monitor the dynamic changes in the gut
21 microbiota, while ^1H NMR profiles were applied to reveal the metabolism of host and
22 microflora. In *Coptis chinensis*-treated group, decreased short chain fatty acids (SCFAs) and
23 branched chain fatty acids (BCFAs) and increased branched chain amino acids (BCAAs) levels
24 were detected in faeces, whereas increased BCFAs were present in the urine. This finding
25 implied that *Coptis chinensis* triggered malabsorption and suppressed bacterial fermentation as
26 well as protein degradation. Meanwhile, decreased levels of *Bacteroides* and *Prevotella* and
27 elevated levels of *Enterobacter* and *Veillonella* in treatment group were significantly correlated
28 to the urinary and faecal metabolites. Using metabolite-set enrichment analysis (MSEA) and the
29 correlation analysis between significant bacteria and metabolites, the results demonstrated that
30 *Coptis chinensis* intervention suppressed glycine and serine metabolism which affected the
31 growth of intestinal bacteria. Moreover, the perturbed microbiome consequently influenced the
32 homeostasis of monosaccharide, amino acid, choline and energy metabolism of gut microbiota
33 and host. These findings help to elucidate *Coptis chinensis* intervention and toxicity;
34 simultaneously, this integrated strategy may provide an effective method for the systematic
35 assessment of host responses to TCM or any other botanical-based nutraceuticals.

36 **Keywords:** *Coptis chinensis* Franch., diarrhea, PCR-DGGE, MSEA, correlation analysis

37 Introduction

38 *Coptis chinensis* Franch. (Huanglian in Chinese, CF), which contains rich alkaloids such as
39 berberine, is a common herb that has been used in traditional Chinese medicines (TCMs) for
40 millennia to treat intestinal infections, particularly bacterial diarrhea.¹ In addition, its
41 cholesterol-lowering and hypoglycemic activities²⁻⁴ against diabetes and obesity have attracted
42 significant interest in the medical field. Nevertheless, there are only a few reports on the
43 mechanisms of its adverse effects, including diarrhea, cardiac damage,⁵ and jaundice,³ resulting
44 from higher doses or long-term treatment with CF. In Chinese clinical reports, diarrhea is one of
45 the most common side effects, with a 19% prevalence rate after CF treatment for diabetes.⁶
46 Diarrhea often occurs in inflammatory and infectious conditions.⁷ Inflammatory diarrhea, which
47 is accompanied by abnormalities in ion transport and mucus secretion, can be found in
48 inflammatory bowel disease (IBD); while infectious diarrhea usually results from exposure to
49 pathogenic bacteria (*Escherichia coli*, *Salmonella*, *Clostridium difficile*, etc.) in a tainted
50 environment or excessive antibiotic use. The types of diarrheas mentioned above are thought to
51 have a close relationship with the maladjusted microflora.^{7,8} Interestingly, our previous study
52 showed that CF-induced diarrhea may relate to the altered gut microbiota via metabonomics
53 analysis of serum and urine.⁵

54 In recent years, botanical-based nutraceuticals have been used as complementary interventions
55 and have been found to improve metabolic syndromes, such as obesity, diabetes or fatty liver
56 disease,⁹⁻¹¹ by regulating maladjusted microbial community. Liquid chromatography-mass
57 spectrometry (LC-MS), gas chromatography-mass spectrometry (GC-MS) and high-resolution
58 NMR spectroscopy (¹H NMR) analysis were widely employed to investigate metabolites in
59 various biological matrixes, including exploring the endogenous mechanism by which the

60 microflora is regulated after berberine treatment in HFD-fed rats. 2 Although the rats exhibited
61 altered amino acids, fatty acids, glutamine and glutamate metabolic pathways, as revealed by
62 urinary and liver metabolic profiles, there was no definitive result that explained which intestinal
63 bacteria contribute to these changes in host's metabolic pathways. Hence, GC-MS combined
64 with pyrosequencing or real-time PCR along with monitoring the blood glucose and lipid levels
65 were applied to interpret the functions of significant bacteria in berberine-treated group. CF and
66 berberine significantly reduced the proportions of faecal *Firmicutes* and *Bacteroidetes* to the
67 total bacteria in high fat diet (HFD)-fed mice.¹² Additionally, *Blautia* and *Allobaculum*, the
68 putative SCFA-producing bacteria, were observed and accompanied with elevated faecal SCFA
69 concentrations. 4 Based on previous studies, we hypothesize that CF-induced diarrhea may be
70 associated with these notable bacteria. Nevertheless, our previous study demonstrated that
71 metabolic profiles of rats with diarrhea were different from the reported profiles. Unfortunately,
72 there is little awareness of whether other bacteria caused this difference and the other side effects
73 of CF that are present when the maladjusted gut microbiota interacts with host.

74 Metabolite-Set Enrichment Analysis (MSEA¹³), an extended approach of gene set enrichment
75 analysis (GSEA¹⁴), applies univariate and multivariate statistical methods to better interpret
76 complex hypothesis-free metabolic signatures based on MS or NMR spectra of the biological
77 samples. This knowledge-based over-representation approach highlights significant pathways
78 that are influenced by xenobiotics or affected by diseases, and shrinkages numerous potential
79 target metabolites. Thus, the elucidation of the pathophysiology or pharmacodynamics
80 mechanism seems to be clearer and more profound. Therefore, Pontoizeau *et al.*¹⁵ revealed
81 homeostasis and physiological plasticity of several inbred strain rats via MSEA, despite their
82 widespread divergences in metabolites and gut microbiota. Because the gut microbiota closely

83 interacts with ingested food in the intestine via fermentation, putrefaction, hydrolysis, and
84 dehydroxylation, changes in different biological matrixes particularly faeces together with the
85 corresponding alternation in the gut microbiota should provide information that can be used to
86 interpret mammalian-microbial interactions. Firstly, antibiotic-treated (AB) animal is
87 indispensable for the study of dysbacteriosis.¹⁶ Swann *et al.*¹⁷ performed fluorescence *in situ*
88 hybridization (FISH) analysis and ¹H NMR spectroscopy in different antibiotic-induced rats that
89 has proven to be feasible methods for ascertaining the influence of the gut microbiota on host's
90 metabolism. In addition, multivariate statistical analyses¹⁶ were applied to reveal the correlation
91 between the perturbed gut microbial community and the changes in faecal metabolites following
92 treatment with different antibiotic, which also explained the function of gut microbiota.

93 Here, we reported a profiling study of urinary and faecal metabolites in SD rats which exposed
94 to an excessive and long-term dose of CF using ¹H NMR, and monitored the fluctuations in gut
95 microbiota via 16S rRNA V3 gene PCR-DGGE. In addition, urine and faecal samples were
96 collected at different time points to characterize the dynamic metabolic profiles resulting from
97 CF administration. Finally, metabolic biomarkers derived from metabonomics analysis were
98 associated with significant bacteria to help clarify diarrhea-associated bacteria in CF-treated rats
99 and to improve our understanding of molecular mechanisms underlying host-microbe
100 interactions at multiple levels.

101 **Materials and methods**

102 **Rat intervention study and sample collection**

103 Fourteen male Sprague-Dawley (SD) rats (8 weeks old, 180-200 g) from the Laboratory
104 Animal Center of Sun Yat-sen University (Guangzhou, P.R. China) were housed at a 12/12 h

105 light-dark cycle with 24 °C and 50-70% humidity. They had free access to water and commercial
106 rodent food unless otherwise specified. After acclimatization for one week, 14 rats were divided
107 equally and randomly into CF-treated and control groups. We implemented animal experiments
108 based on the Institutional Animal Care and Use Committee (IACUC) of Sun Yat-sen University
109 and the *Coptis chinensis* decoction was prepared according to a previously reported standardized
110 protocol.⁵ Rats in control group were subjected to gavage with distilled water, while CF-treated
111 rats were orally administered at a dose of 5 g/kg weight decoction of *Coptis chinensis* for 14
112 consecutive days, respectively. The dosage was determined based on the reference to the Chinese
113 Pharmacopoeia (10 g per human per day, version 2010) and our pre-study results, and at this
114 dosage we observed the main side effect is diarrhea. Urine and faeces Samples were collected in
115 Eppendorf tubes on ice from 8:00 to 16:00 on pre-dose day 1 and post-dose day 7, 14, 21. The
116 fresh samples from each group were stored at -80 °C for NMR and microbiological analyses.

117 **Sample preparation for NMR spectroscopy**

118 Urine samples were thawed on ice and 600 µL was mixed with 60 µL of phosphate buffer/
119 D₂O (1.5 M Na₂HPO₄-NaH₂PO₄, pH 7.4). The buffer contains 0.1% of NaN₃ to avoid bacterial
120 contamination and 0.05% TSP to afford a field-frequency lock. The mixtures were centrifuged at
121 16000 g at 4 °C for 10 min to remove any sediment. Faecal extraction used the optimized
122 method described by Wu et al.¹⁸ The 600 µL coalescent supernatant was pipetted into 5 mm
123 NMR tubes and 1D ¹H NMR spectra were obtained using a Bruker AVIII 600 MHz spectrometer
124 (Bruker Biospin, Germany) at 600.13 MHz and 298 K. The standard pulse sequence (NOESY)
125 with water presaturation for urine and faecal spectrums also referred to prior study.¹⁸ 2D NMR
126 experiments, including total correlation spectroscopy (TOCSY), *J*-resolved spectroscopy (JRES)
127 and ¹H-¹³C HSQC, were performed on selected samples to assign the NMR spectra of the

128 metabolites. The metabolites were simultaneously identified based on the Human Metabolome
129 Database (<http://www.hmdb.ca/>) and metabonomics toolbox (Chenomx NMR Suit 7.6,
130 Chenomx, Canada) as well as published work.^{19,20}

131 All ¹H NMR spectra were manually phase and baseline-corrected and calibrated to TSP at 0.00
132 ppm using TOPSPIN (V2.1, Bruker Biospin). The spectral region (0.5-9.50 ppm) was segmented
133 into 0.004 ppm chemical shift bins using the AMIX package (V3.9.14, Bruker Biospin). For
134 urine samples, the water signal (4.70-4.95 ppm) and urea signal (5.50-6.25 ppm) were removed
135 prior to analysis. The water signal (4.68-4.95 ppm) in faecal extracts was also discarded to
136 exclude the efficient water suppression. All remaining regions were normalized to the total
137 integrated spectrum before multivariate data analysis.

138 **Molecular biological analysis and data processing**

139 Total bacterial DNA was extracted from faecal samples using a TIANamp Stool DNA Kit
140 (Tiangen, Beijing, P.R. China) in accordance with the manufacturers' instructions with slight
141 modification and then stored at -20 °C for further analysis. Universal primers 357f_GC clamp
142 and 518r targeted the hypervariable V3 region of the 16S rRNA gene and were used to conduct
143 PCR amplification. Initial denaturation was at 95 °C for 3 min, and then a total 25 cycles
144 including denaturation at 95 °C for 1 min, annealing at 55 °C for 1 min, extension at 72 °C for 1
145 min, and a final extension at 72 °C at 8 min. After confirmation using agarose gels
146 electrophoresis, the PCR products were analysed with a 38-58% gradient DGGE under constant
147 voltage of 70 V for 13 h at 60 °C in 1 × Tris-acetate-EDTA (TAE) buffer using the DCode
148 universal mutation detection system (Junyi, Beijing, P.R. China). Silver staining was performed
149 to visualise the changing profile in predominant bacterial profiles and this fingerprint was

150 recorded by a digital camera (Canon, Japan). DGGE images were converted to black-and-white
151 using Adobe Photoshop CS4, and digitized by Quantity One software (version 4.6.2). The
152 relative band intensity was exported as a data matrix for normalization prior to pattern
153 recognition analysis. Meanwhile, the auto search option was used to mark individual bands of
154 each sample lane, followed by necessary manual correction.

155 *Statistical analysis and metabolite-strain correlation networks*

156 Multivariate data analysis was conducted by SIMCA-P+ (version 12.0 Umetrics, Sweden) and
157 SPSS software (V20.0, Chicago, USA). The unit variance (UV)-scaled NMR data and DGGE
158 data were analysed separately with principal component analysis (PCA) to investigate the
159 intrinsic similarity or dissimilarity as well as possible outliers in each matrix. Following partial
160 least squares (PLS) and orthogonal projection to latent structure-discriminant analysis (OPLS-
161 DA), the model was validated using a 7-fold cross-validation method and 200 permutation tests,
162 as well as further assessment using CV-ANOVA tests, with a significant level of $p < 0.05$. The
163 color-coded loading plots were carried out in MATLAB (The Mathworks Inc.; Natwick, MA,
164 version 7.1) based on correlation coefficient values to interpret important metabolites that
165 contribute to the class separation. Meanwhile MSEA²¹, an approach to assess whether significant
166 metabolites found in known metabolic pathway maps or databases coincide with the metabolic
167 signature at a certain level of the biochemical pathway, was applied to reduce the massive
168 number of insignificant metabolic pathways. Finally, the covariation analysis between ¹H NMR
169 and DGGE data were integrated by O2PLS²² modeling and Pearson's correlation coefficient²³
170 calculation. NMR peaks or DGGE bands with $Q^2 > 0.6$ and $|r| \geq 0.755$ were selected to exhibit a
171 bio-network with the Gephi 0.8.2 software.²⁴

172 Cloning and sequencing of specific bands

173 Bands that were closely correlated with metabolites in the two groups were excised and
174 subjected to further identification by sequencing. Rinsed DNA bands were dissolved in 25 μ l TE
175 buffer for 16 h at 4 $^{\circ}$ C, and then amplified with universal V3 primers without GC clamp. The
176 positive clones were purified and verified as described in previous study.²⁵ After sequencing
177 (Sangon Biotech, Shanghai, China), the results were assembled with Chromas software for
178 homology searches in NCBI GenBank databases using the BLAST tool. Based on BLAST
179 results, reference sequences of phylogenetic neighbor species (up to 90% similarity) were
180 included to confirm the allocation of the purified band sequences to the most probable species.
181 The sequences were deposited in GenBank with the following accession numbers: KR 611915-
182 611917, KR 708629 and KR 611919-611922.

183 Results and Discussion

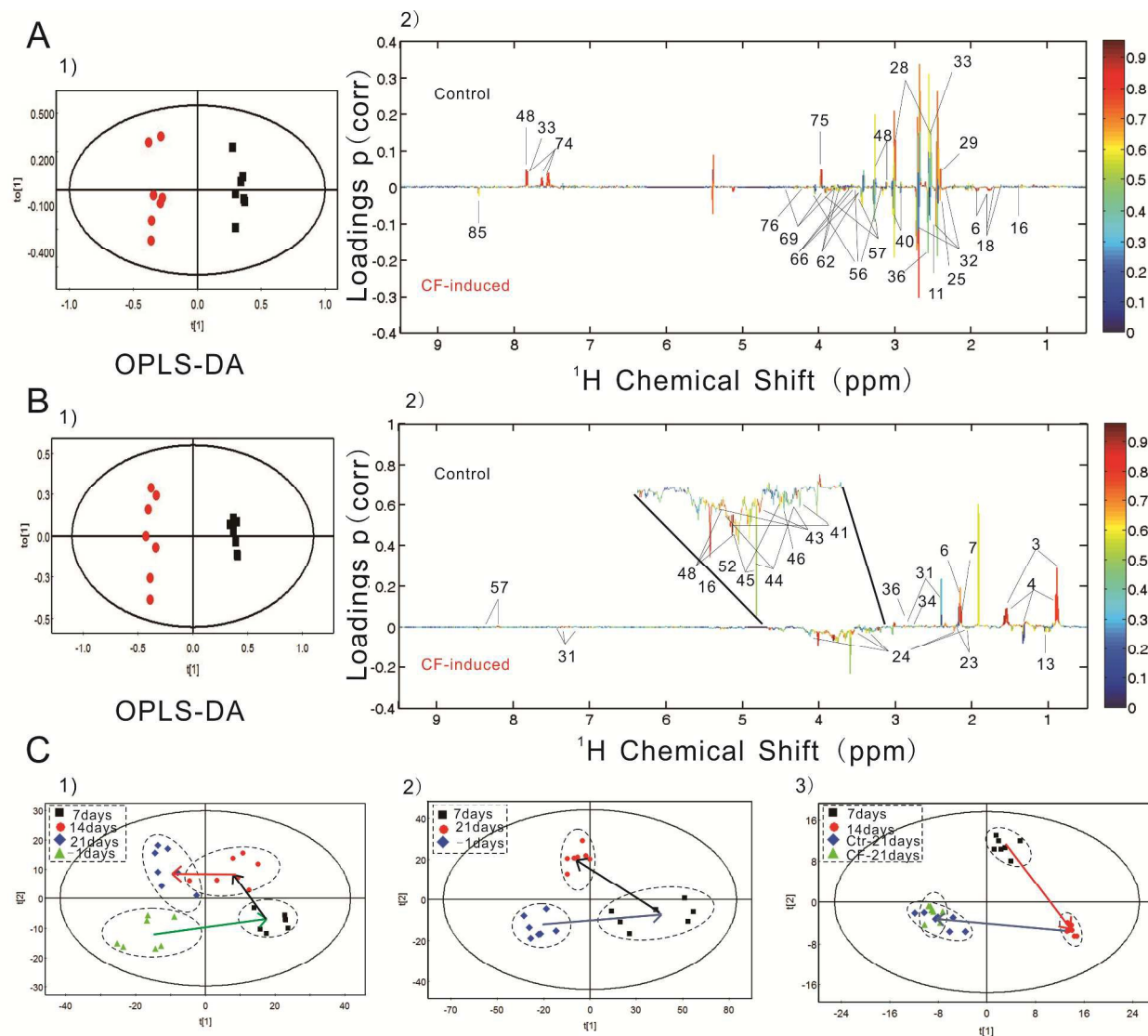
184 Metabolic changes in urine and faeces following the CF intervention

185 CF-treated rats displayed diarrhea after 6 days of oral administration and recovered at 7 days
186 after intervention. CF-induced rats also exhibited growth suppression compared to control group,
187 similar to our previous study.⁵ From NMR metabolic profiles, we detected 85 metabolites in
188 urine samples and 58 components in faecal solutions after CF consumption by combining CF-
189 induced group with control group (Supplementary Figure S1). The signals from urine mainly
190 contained glucose, glycogen, amino acids, amines, organic acids, TCA intermediate metabolites
191 such as citrate, 2-oxoglutarate, succinate and fumarate, and a series of SCFAs. Faecal spectra
192 were mainly comprised of amino acids, glucose, hemicellulosic sugars (arabinose and xylose),

193 some keto acids (*e.g.*, α -ketoisovalerate and α -ketoisocaproate), as well as amines and SCFAs.
194 The specific NMR assignment can be found in Supplementary Table S1 and S2.

195 Subsequently, spectra signals were converted into a digital matrix for statistical analysis, which
196 could reveal more detailed information about the CF-induced metabonomic changes. Compared
197 with analysis of day -1 of control and CF-treated group, we found an obvious discrimination
198 between control rats and CF-treated rats on day 7 using PCA model (Supplementary Figure S2A,
199 B). In addition, OPLS-DA models for urinary profile ($R^2X = 0.528$, $Q^2 = 0.836$) and faecal
200 extract spectra ($R^2X = 0.786$, $Q^2 = 0.963$) on day 7 were used to investigate the differences in
201 metabolic concentrations between samples which obtained from CF-induced rats and the
202 matched controls. The OPLS-DA scores plots and the coefficient loading plots (Figure 1A, B)
203 illustrated that the CF intervention significantly altered metabolites induced by CF intervention.
204 As Jiang et al.^{26,27} reported, organ especially liver concentrations of berberine or its metabolites
205 was 10-fold or 30-fold higher than that in plasma, whereas only 0.0939% and 22.74% recovered
206 rate of berberine in urine and feces after oral administration. It is worth mentioning that the
207 differentiation occurred in control group at day -1 and day 7 (Supplementary Figure S2C, D)
208 which suggested that dietary and gavage cause the overall metabolic alteration in control rats
209 over time. To minimize unpredictable factors, we reviewed those biomarkers found on day 7. In
210 addition to verification with VIP values, Student's t-test was used to analyse authentically
211 different metabolites by comparing control samples at day -1 and day 7. Finally, 21 significantly
212 different metabolites in urine samples were sorted out. Those discarded components which
213 expressed differentially in the control group were supposed to have little association with CF
214 administration. Similarly, after removing hypocritical biomarkers from faecal extract solutions,
215 we noticed that 9 faecal metabolites showed significantly lower NMR response after CF

216 perturbation, whereas 10 metabolites in faeces displayed the opposite behavior as shown in
 217 Figure 1.



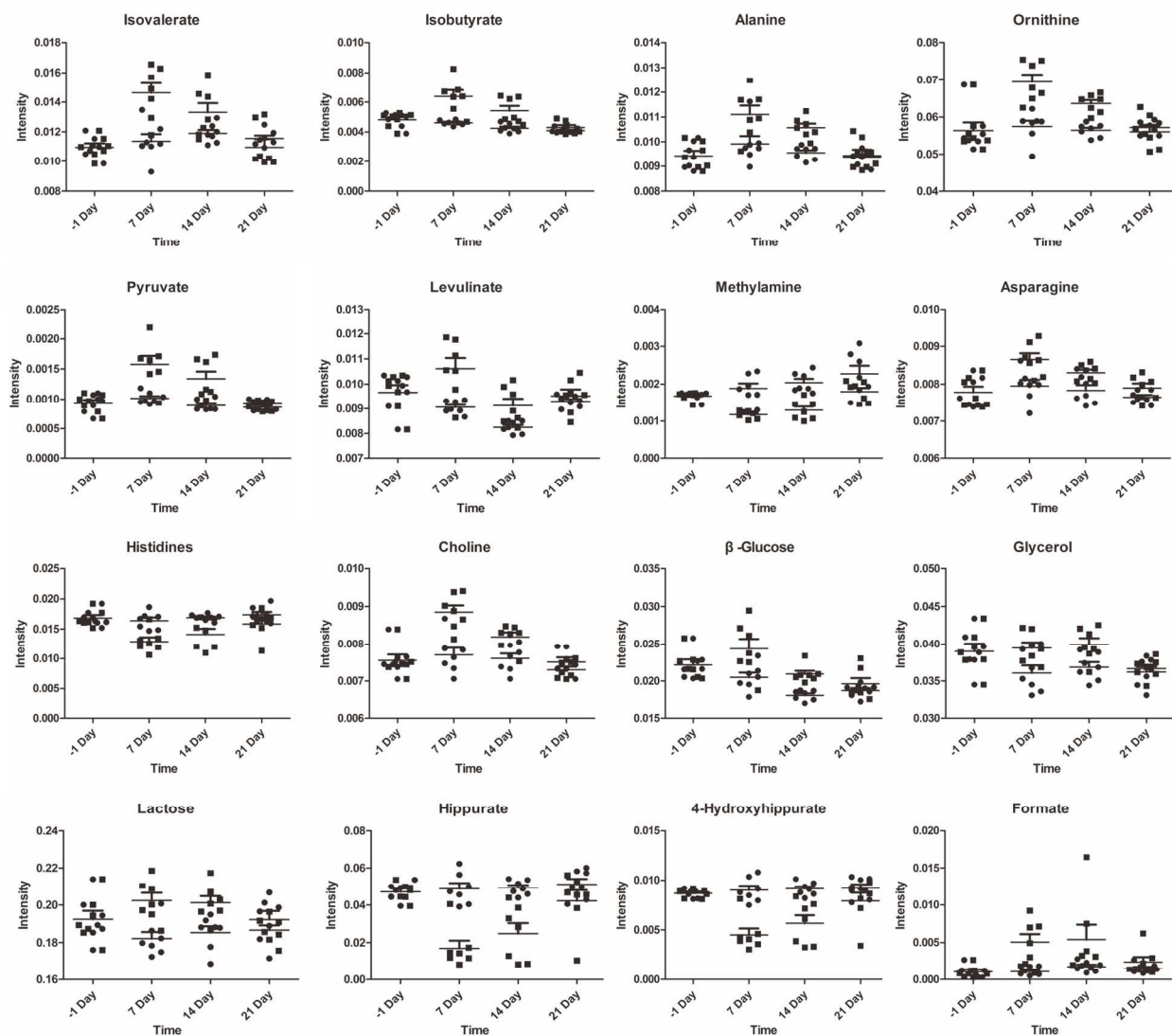
218
 219 **Figure 1** ¹H NMR coefficient loading profiles from OPLS-DA model on day 7 and PLS-DA
 220 scores plots with time-dependent trajectory. A is for urine samples, B is for faeces and in C
 221 graph: (1), (2), (3) exhibit fluctuations of 4, 3, 3 time points in urine, faeces and microbiota
 222 respectively.

223 To investigate the time-dependence and recoverability of the CF effects, we analysed the CF-
224 induced urinary and faecal metabolic alterations at four and three time points respectively
225 (Figure 1C). PLS-DA scores plots ((1) $R^2X = 0.327$, $Q^2 = 0.402$; (2) $R^2X = 0.621$, $Q^2 = 0.906$;
226 (3) $R^2X = 0.776$, $Q^2 = 0.973$) showed the specific profiles in the CF-induced group on the
227 selected days. Once the diarrhea occurred, the metabolic trajectories of host and gut microbiota
228 diverged from their initial metabolic position. After 7 days (on day 21) of recovery, we found
229 their metabolic profiles returned to approximately the pretreatment level. On the other hand,
230 using microbial profiles in faecal samples obtained from DGGE analysis, the CF-induced
231 fluctuations in the composition of gut microbiota were in accord with the faecal metabolic
232 changes (Figure 1C).

233 **Altered metabolites in urinary and faecal samples are related to CF intake**

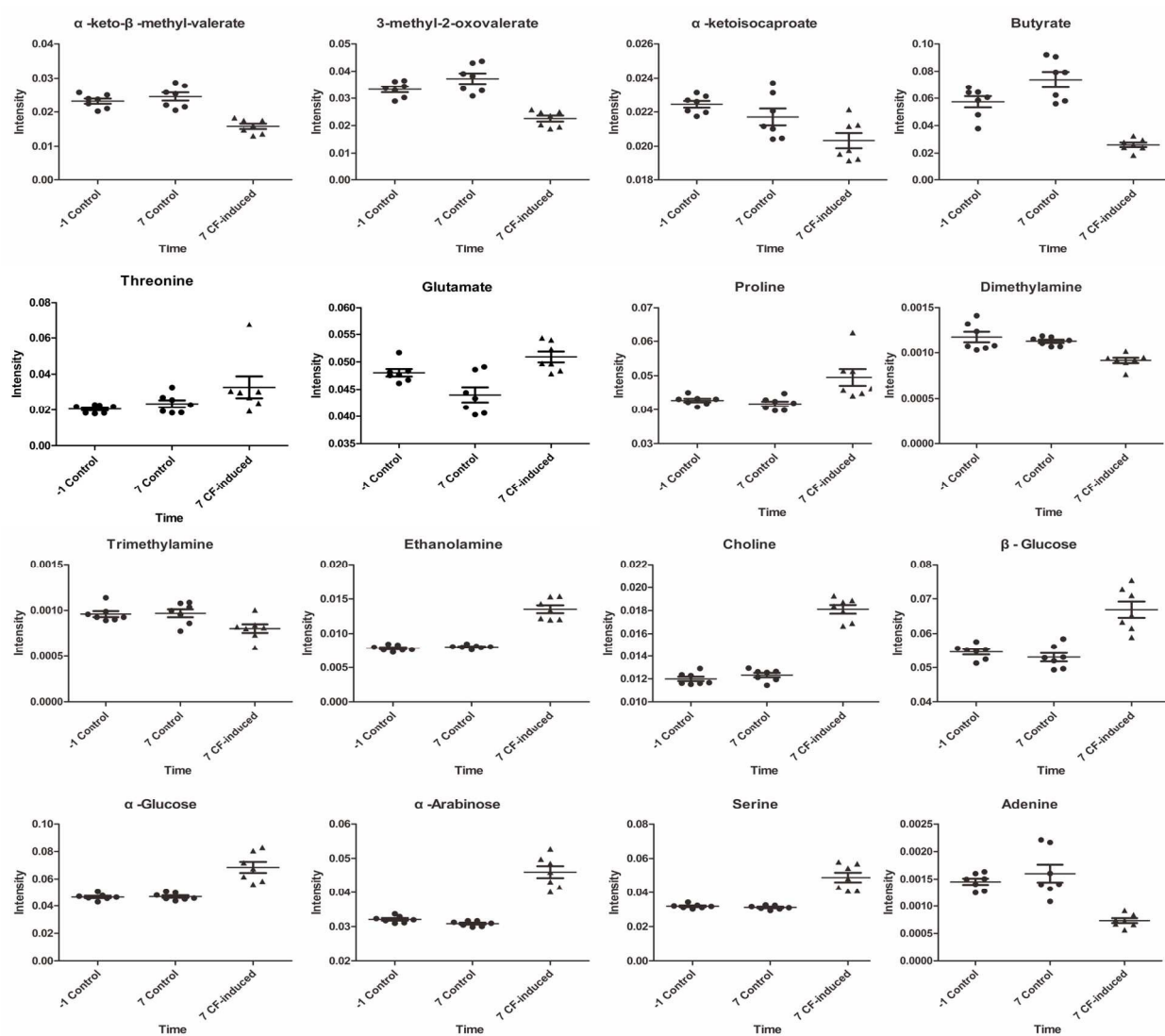
234 In Figure 2, significant metabolites in urinary metabolic profile were investigated following
235 treatment and during convalescence, and compared to predose profiles. Alanine, pyruvate and
236 glucose, which are involved in alanine-glucose cycle,²⁸ displayed increased levels in CF-induced
237 group. Elevated levels of choline and glucose were also found in a number of CF intervention
238 urine samples, which were similar to faecal samples (Figure 3). Branched chain fatty acids
239 (BCFAs) especially isobutyrate, isovalerate, and 2-methylbutyrate are products from oxidation of
240 valine, leucine, and isoleucine, respectively.²⁹ It is also believed that colonic bacteria are capable
241 of decomposing proteins, peptides, and amino acids to produce BCFAs,³⁰ as well as SCFAs.
242 What surprised us is that there were higher levels of BCFAs particularly isobutyrate and
243 isovalerate in CF-administered rats compared to controls, but these differed from faecal
244 metabolism. The increased BCFAs in urine samples implied that host increased BCFAs
245 absorption following CF stimulation to maintain energy balance. Whereas, decreased BCFAs

246 and increased BCAAs of faecal samples suggested that the BCFA-BCAA (branched chain amino
247 acid) pathway has been disturbed, in that the maladjusted gut microbiota decreased the utilization
248 of BCAA to produce BCFA. It is remarkable that urinary hippurate, as a gut microbial-
249 mammalian co-metabolite that is generated from aromatic compounds and polyphenolics by gut
250 microbes,³¹ was obviously reduced in rats with diarrhea. The dysbiosis of the gut microflora in
251 treated rats not only related to imbalanced SCFAs in faeces but also reflected the decreased
252 hippurate in the urine.



253

254 **Figure 2** Distributions of intensities for selected urinary metabolites based upon the normalized
 255 bucket table. Significant metabolites of rats' urine which compared control group with CF-
 256 treated group at different time points: day -1 is pre-administration day, day 7 and day 14 are
 257 diarrhea days, and day 21 is post-administration day for 7 days.



258 **Figure 3** Distributions of intensities for selected faecal metabolites based upon the normalized
 259 bucket table. Significant metabolites of faeces samples from CF-treated group were compared
 260

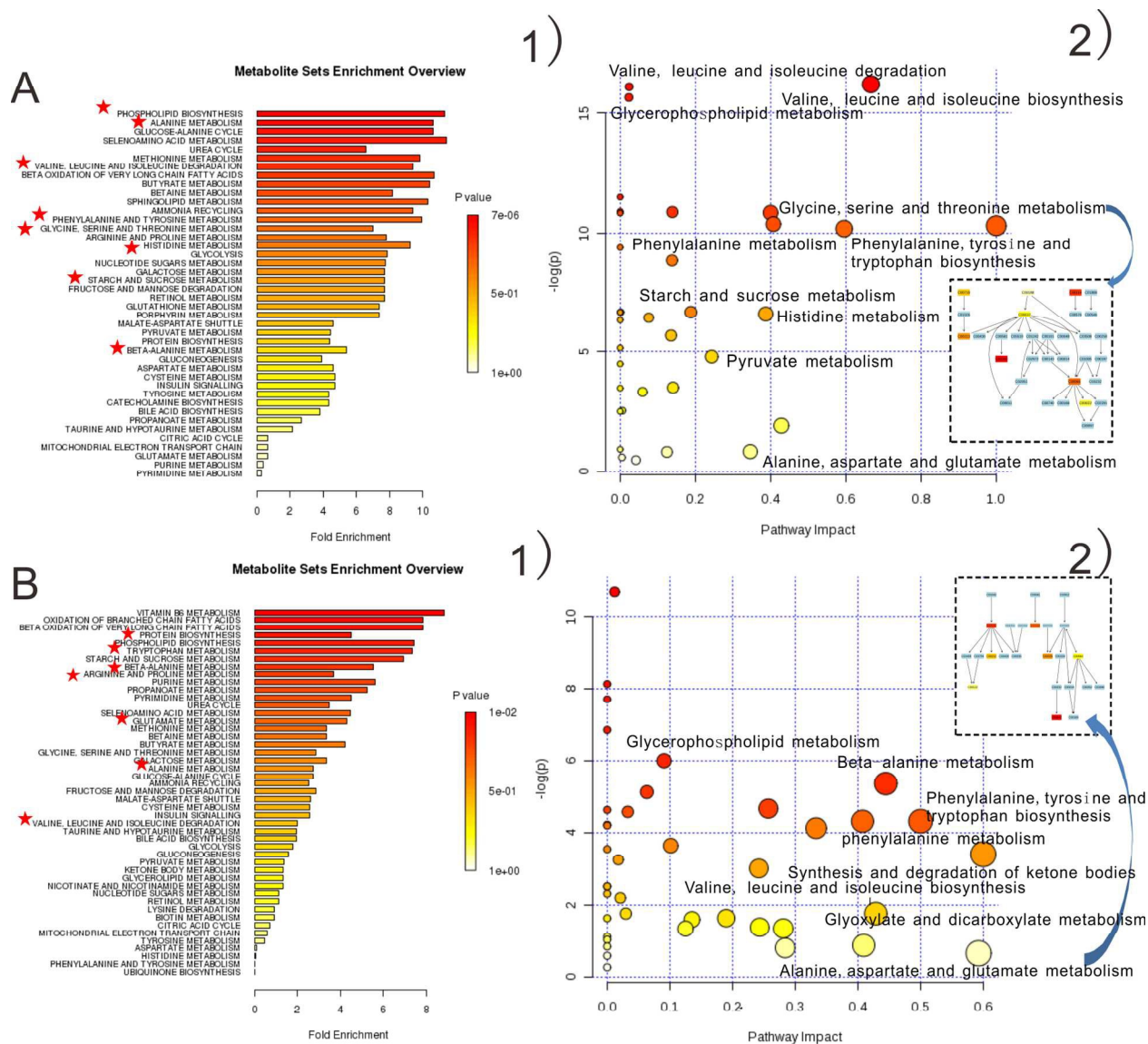
261 with control group ones at different time points: day -1 is pre-administration day, day 7 is
262 diarrhea at the first day.

263 The faecal metabolic profile (Figure 3), which is a direct reflection of changes in microbial
264 composition due to the CF intervention, showed altered faecal metabolites with previous VIP
265 value sifting and t test ($p < 0.05$). Butyrate, the most important component of SCFAs, plays a
266 crucial role as an energy source for colon cells.³² Moreover, butyrate provides ATP, which
267 participates in $\text{Na}^+\text{-H}^+$ exchange to promote absorption of water and sodium,³³ and this
268 facilitates foundation of the anti-diarrhea hypothesis. In this study, the significantly reduced
269 butyrate level in CF-treated rats may be closely associated with suppressed butyrate-producing
270 bacteria. Choline metabolites such as dimethylamine and trimethylamine, which often modulate
271 lipid metabolism and glucose homeostasis,^{34,35} had a similar decreasing trend in the group with
272 diarrhea. In contrast, choline level was not consistent with the dynamic change in its metabolites,
273 and instead showed an increase. We speculated that the CF-induced dysbiosis of gut microbiota
274 impaired choline metabolism. On the other hand, the elevated level of ethanolamine from choline
275 pathway is able to facilitate lecithin synthesis and preserve cellular integrity, because
276 cytomembrane consists of lecithin.³⁶ As we know, α -keto acids derived from deamination of α -
277 amino acids can form nonessential amino acids or offer energy for host through complete
278 oxygenolysis; while glucogenic amino acids are able to transform into glucose.²⁸ Interestingly,
279 we observed that α -keto acids such as 3-methyl-2-oxovalerate, α -keto- β -methyl-valerate, α -
280 ketoisocaproate, and α -ketoisovalerate, were depleted levels in CF-treated group, whereas some
281 amino acids were consistent with the elevated level of glucose. Therefore, we tentatively
282 hypothesize that these results act as one factor that promotes the growth suppression of CF-
283 treated rats in the current study. Although, some urinary and faecal biomarkers have been found

284 to be influenced by the CF intervention, there was no distinct identification of the systematic
285 changes in host.

286 **MSEA focused on meaningful signaling pathways that regulate metabolism**

287 MSEA¹³ is often applied to quantitative metabolomic data for identifying and interpreting
288 changes in human or other mammalian pathway-associated metabolite concentrations. According
289 to previous studies,^{21,37} we aimed to determine which pathways were dramatically affected based
290 on the detected metabolites. Enrichment tests with a qualitative overrepresentation analysis or a
291 quantitative enrichment analysis were performed, and numbers of potential target metabolites
292 from KEGG database (<http://www.genome.jp/kegg/>) were swift reduced into a set of particular
293 metabolic pathways (Figure 4 and Table ~~S2~~, S3, S4, S5 and S6). From metabolite sets
294 enrichment profiles and pathway impact illustrations, we focused on 10 significant pathways in
295 urinary and faecal samples. Remarkably, they shared 5 pathways to some extent, although
296 metabolites involved in these shared pathways were not absolutely uniform.



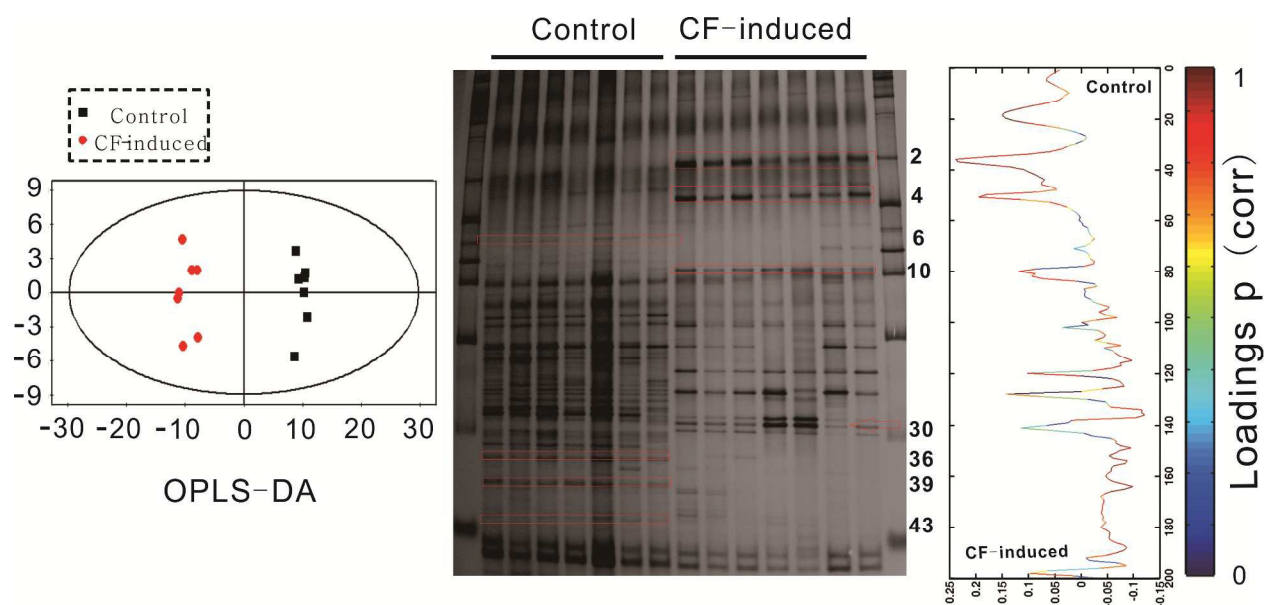
304 In this study, urinary pathways of host and faecal pathways of intestinal microbiome had an
305 interconnected role in energy metabolism. For instance, pyruvate metabolism, the core of TCA
306 cycle, showed difference in CF-treated faeces. As we know, TCA cycle is the common and
307 ultimate pathway for the oxidation of carbohydrates, fatty acids, and amino acids³⁸ that connects
308 with numerous other pathways. Alanine, aspartate, and glutamate degradation include TCA
309 intermediates such as 2-oxoglutarate, citrate, and succinate showed suppression in urinary
310 samples, as well as glyoxylate and dicarboxylate metabolism. Furthermore, starch and sucrose
311 metabolism was disturbed in view of increased glucose level. These results indicated that host
312 and gut microbiota interacted to maintain balance of energy metabolism via some important
313 metabolic intermediates when suffered from excessive CF. Meanwhile, the maladjusted gut
314 microbiota may relate with some perturbed amino acids pathways. Valine, leucine and isoleucine
315 metabolism were altered in both faeces and urine. Increased leucine and valine levels indicated
316 that their biosynthesis restrained its degradation, and the homologous keto acids such as α -keto-
317 β -methyl-valerate and α -ketoisovalerate, were subsequently decreased. In addition, succinate was
318 affected by the aberrant metabolism because it requires valine and leucine to take part in TCA
319 cycle.³⁹ Excessive and long-term dose of CF not only cut down the energy supplement of host
320 and gut microbiota, it may also tempt invasive bacteria to worsen the systemic metabolism.
321 Aromatic amino acid metabolism includes phenylalanine, tyrosine and tryptophan metabolism,
322 and is required to produce neurotransmitters; it is believed that this gut microbiota-host co-
323 metabolism is associated with the gut-brain axis (GBA).⁴⁰ The GBA seems to modulate
324 homeostasis of gastrointestinal (GI) tract function once the central nervous system induces
325 changes or the GI tract alters the habitat and perturbs the gut microbiota, because the habitat of
326 the microbiota depends on GI motility and epithelial functions. Significant decrease levels of

327 hippurate and 4-hydroxyhippurate at day 7 and day 14 in the CF-induced group while the
328 elevation at day 21 were observed in urine, which suggested that phenylalanine pathway affected
329 GI tract function and disturbed gut microbiota. However, decreased 2-oxoglutarate level and
330 increased urea and asparagine levels involved in alanine, aspartate and glutamate metabolism
331 demonstrated that excessive CF did not injure the liver and kidney of rats, in that the metabolism
332 correlates with the liver and kidney functions about ammonia transportation.²⁸ Changes in
333 glycine, serine and threonine metabolism (Figure 4A-2), the additional block scheme) were
334 noticed for glycine, which belongs to the choline degradation pathway and is degraded into
335 creatine through betaine and *N, N*-dimethylglycine.⁴¹ Additionally, glycine and serine can be
336 transformed into one carbon unit which is indispensable for the synthesis of purine and pyridine.
337 ²⁸ We found this metabolism was suppressed, which supposed to be the reason that some
338 intestinal bacteria growth was restrained. At the same time, we noticed that phosphorylcholine
339 level in choline degradation pathway increased while dimethylamine and trimethylamine
340 obtained from microbes degradation was dramatically reduced. In short, these aberrant
341 metabolites or pathways were deemed to correlate with altered intestinal bacteria.

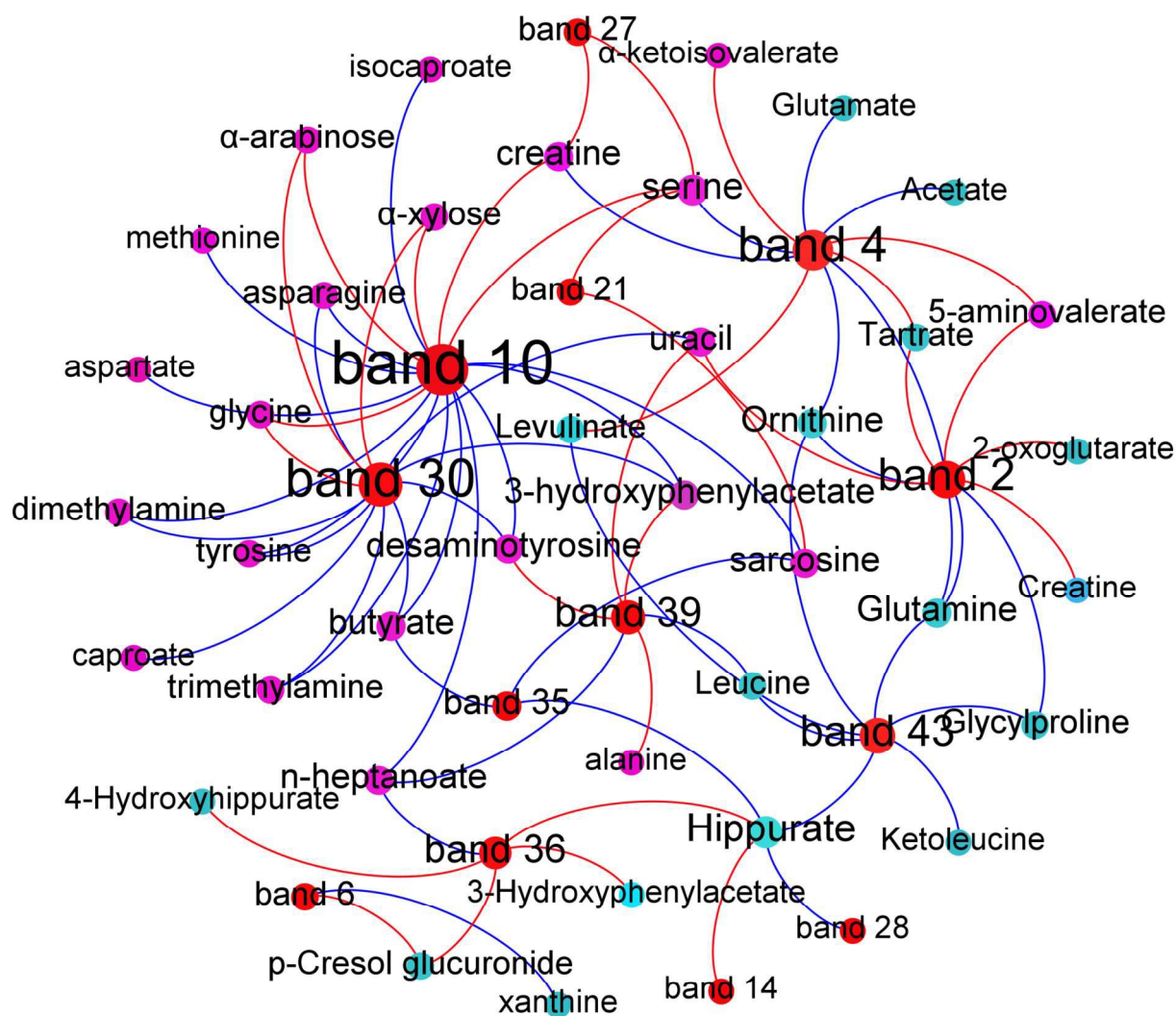
342 **Gut microbial markers in CF-induced rats**

343 To investigate CF-induced fluctuations in rats' gut microbiota, we performed DGGE analysis
344 to visualize microbial diversity in faecal samples collected on day 7. R^2X and Q^2 values from
345 OPLS-DA model (Figure 5) of digital DGGE gel are 0.564 and 0.907 respectively, which
346 provided a good prediction of discriminating groups. We observed approximately 45 bands, and
347 then integrated 1H NMR spectral data with DGGE microbial data using O2PLS. Thirteen
348 differential bands were associated with significant metabolites (Figure 6); and only 8 particularly
349 prominent bands were selected for cloning and sequencing (Table 1). (Due to segmentary

350 correlations with sporadic metabolites, the 5 residual bands have not been probed in following
 351 discussion.) Although the number of bands in CF-treated group has been significantly reduced,
 352 there were 4 bacterial species that arose in rats with diarrhea and 4 bacteria in control group that
 353 appeared to correlate with important metabolites. Using BLAST analysis, we obtained bacterial
 354 species or phylotypes which were confirmed by clustering analysis, and there were one Firmicute
 355 (*Veillonella parvula*), one Bacteroidete (*Bacteroides vulgatus*), and two Proteobacteria species
 356 (*Acidovorax avenae* and *Enterobacter aerogenes*) in CF-treated group, while 4 species from
 357 control rats belonged to Bacteroidete.



358
 359 **Figure 5** 16S rDNA PCR-DGGE on day 7, the red marked bands are significant in diarrhea
 360 progressing. OPLS-DA coefficient loading profile (right) displayed the discriminative DGGE
 361 bands by comparing the treated group with control.



362

363 **Figure 6** Correlation network between altered DGGE bands (the corresponding bacterial species
 364 in Table 1) and changed metabolic components of rats' urine and faeces visualized with Gephi.
 365 This map calculated using Pearson correlation coefficients ($|r| \geq 0.755$ and $p < 0.05$), and node
 366 size denotes the highest effect size for each band or metabolite comparing treated group with
 367 control group. Nodes colored red for bands, amaranth for faecal metabolites and cyan for urinary
 368 ones. Red lines correspond to positive correlations, whereas blue lines correspond to negative
 369 correlations.

370 **Table 1** Closest relatives of 16S rDNA V3 regions sequences derived from DGGE bands.

DGGE band	Sample	Seq. length(bp)	domain	phylum	class	order	family	genus	species	S_ab score	Accession Numbers
Band 2	CF	189	Bacteria	Bacteroidetes	Bacteroidia	Bacteroidales	Bacteroidaceae	<i>Bacteroides</i>	<i>Bacteroides vulgatus</i>	1.00	KR611915
Band 4	CF	194	Bacteria	Proteobacteria	Betaproteobacteria	Burkholderiales	Comamonadaceae	<i>Acidovorax</i>	<i>Acidovorax avenae</i>	0.90	KR611916
Band 6	Ctr	189	Bacteria	Bacteroidetes	Bacteroidia	Bacteroidales	Prevotellaceae	<i>Prevotella</i>	<i>Prevotella dentalis</i>	0.96	KR611917
Band 10	CF	194	Bacteria	Proteobacteria	Gammaproteobacteria	Enterobacteriales	Enterobacteriaceae	<i>Enterobacter</i>	<i>Enterobacter cloacae complex</i>	0.96	KR708629
Band 30	CF	195	Bacteria	Firmicutes	Negativicutes	Selenomonadales	Veillonellaceae	<i>Veillonella</i>	<i>Veillonella parvula</i>	0.94	KR611919
Band 36	Ctr	190	Bacteria	Bacteroidetes	Bacteroidia	Bacteroidales	Prevotellaceae	<i>Prevotella</i>	<i>Prevotella denticola</i>	0.94	KR611920
Band 39	Ctr	189	Bacteria	Bacteroidetes	Bacteroidia	Bacteroidales	Bacteroidaceae	<i>Bacteroides</i>	<i>Bacteroides helcogenes</i>	0.94	KR611921
Band 43	Ctr	189	Bacteria	Bacteroidetes	Bacteroidia	Bacteroidales	Bacteroidaceae	<i>Bacteroides</i>	<i>Bacteroides vulgatus</i>	0.99	KR611922

371 CF, CF-induced group; Ctr, control group.

372

373 CF-induced intestinal bacteria dominated the fluctuation in urinary and faecal metabolites

374 The maintenance of human health and the occurrences or developments of disease are deemed
375 to have close relationship with gut microbiota. To ascertain the complicated interaction between
376 host and microbes, we integrated ^1H NMR spectral data and DGGE microbial data to
377 demonstrate the mechanism of CF-induced diarrhea (Figure 6). In rats with diarrhea, we found
378 that the dysbiotic signature was highly characteristic for the abundant emergence of *Enterobacter*
379 *aerogenes* (band 10) and *Veillonella parvula* (band 30), which correlated with numbers of faecal
380 metabolites. *Enterobacter aerogenes* is a normal bacterium and often inhabits in the mammalian
381 intestine, and it is believed to be linked with the occurrence of colicky in infants.⁴² In the
382 correlation map, *Veillonella parvula*, a member of the most active microflora that participates in
383 immunoregulation,⁴³ such as *Enterobacter*, had similar interactions with perturbed metabolites.
384 Two other invasive bacterial species in CF-induced rats were *Bacteroides vulgatus* (band 2) and
385 *Acidovorax avenae* (band 4), both of which interfered urine and faeces metabolism. *Acidovorax*
386 *avenae* is abundant in plant, but some researchers reported that *Comamonadaceae* including
387 *Acidovorax* were decreased in the gut of high weight hosts.⁴⁴ Interestingly, the suppressed
388 growth of CF-treated rats exactly correlated with increased *Acidovorax avenae*; once the animals
389 resumed their growth, this bacterium was dramatically reduced (Figure S3). *Bacteroides*, which
390 are obligatory anaerobic bacteria, are important for food digestion because they are rich in
391 carbohydrate transport and protein-metabolism-related enzyme, and contain glycan, vitamins,
392 and cofactor enzymes.⁴⁵ Bacteria from Bacteroidetes are the predominant and most robust
393 bacteria in the gut of conventional mice, which was ultimately confirmed by our results.
394 Excessive CF impeded these dominant bacteria (band 6, 36, 39 and 43), while the relevant
395 metabolism of CF-induced rats recovered after terminating the intervention.

396 **Gut microbiota affected carbohydrates metabolism.** It is known that the gut microbiota
397 convert monosaccharide into SCFAs by fermentation,⁴⁶ and SCFAs are absorbed to supply
398 energy and nutrients to the host and microbes.⁴⁷ In our study, *Enterobacter aerogenes* and
399 *Veillonella parvula* showed strong positive correlations with monosaccharides such as α -xylose
400 and α -arabinose, but exhibited a negative relevance with SCFAs (butyrate, caproate and
401 isocaproate). SCFAs particularly butyrate, also have immunomodulatory effects that prevents the
402 gut from the inflammation.⁴⁸ The fact that α -xylose and α -arabinose were elevated and SCFAs
403 were decreased in faeces may indicate that bacteria responsible for monosaccharide glycolysis
404 were suppressed and the inflammation that accompanies diarrhea cannot be alleviated. *Prevotella*,
405 the abundant genera of host gut, whose relatives are rich in xylanase, carboxymethylcellulase
406 and endoglucanase^{49,50} in the rumen, may supply a 'permissive' gut microbiota to produce high
407 levels of SCFAs.⁵¹ However, it did not show a close relationship with SCFAs in this map, but
408 some reports demonstrated that abnormal fluctuations in *Prevotella* have been found in various
409 intestinal diseases such as IBD^{52,53} and diarrhea⁵⁴, which occurred in our study.

410 **Gut microbiota affected amino acid metabolism.** Combined with the metabolic biomarker
411 and significant pathways mentioned above, we found that the imbalanced gut microbiota
412 severely impaired amino acids metabolism but interacted with different directions for host and
413 themselves. 5-aminovalerate is the intermediate of lysine degradation by gut microbiota,⁵⁵ which
414 is then metabolized into acetate and propionate. In our study, there was no relationship between
415 band 2 and saccharides, except for 5-aminovalerate. Similarly, band 4 showed a positive
416 correlation with 5-aminovalerate but negative relevance with urinary acetate. Therefore, the
417 energy deficiency of host in response to decreased SCFAs may relate to the increase in band 4.
418 Alanine, aspartate and glutamate metabolism including faecal aspartate and asparagine levels,

419 were negatively correlated to band 10 and urinary glutamine negatively correlated with band 2,
420 band 4 and band 43. CF-induced bacteria are supposed to hamper the energy metabolism because
421 alanine metabolism is closely related to TCA cycle. In correlation map, we observed that
422 metabolites such as ornithine and aspartate in arginine and proline metabolic pathway displayed
423 negative correlations with band 2, band 4 and band 43 or band 10. As we know, *Bacteroides*
424 convert mucoitin into proline⁵⁶ which is enriched in glycoprotein of intestinal epithelial cells.⁵⁷
425 Proline is increased in colorectal cancer patients,⁵⁸ and our results revealed a similar elevation in
426 the CF-treated rats. This may reflect that CF-induced diarrhea impaired morphology and function
427 of colonic epithelial cells. In previous studies, *Bacteroides vulgates* displayed a reduction in
428 patients with IBD^{59,60} and diarrhea,⁶¹ but it showed a significant increase in our group with
429 diarrhea. The result demonstrated that the dysbiosis in CF-induced diarrhea differs from the gut
430 imbalance of IBD. Phenols are rich in our daily diet. After deglycosylation, dehydroxylation and
431 demethylation by the gut microbiota,⁶² they are converted to *p*-cresol and phenol in the systemic
432 circulation or excretion.⁶³ Interestingly, 3-hydroxyphenylacetate and *p*-cresol glucuronide were
433 positively correlated with the abundance of *Prevotella*, as well as hippurate and 4-
434 hydroxyhippurate. Urinary hippuric acid is believed to have an association with tyrosine and
435 phenylalanine in faeces, in that the microbiota produces hippuric acid by the catabolism of these
436 amino acids.⁶⁴ Moreover, faecal hydroxyphenylacetic acid, which is produced from tyrosine
437 through microbial enzymes, showed the same correlation with band 10 and band 30 as tyrosine.
438 Our result suggests that excessive CF administration impaired the bacterial-mediated synthesis
439 and then impaired host metabolism when the elevated phenylalanine level was compared with
440 decreased phenylpropionate, hydroxyphenylacetate, hippurate and hydroxyhippurate levels. In
441 conclusion, long-term excess CF use impaired the gut-host co-metabolism.

442 **Gut microbiota affected choline metabolism.** The prominent findings were the suppression
443 of bacterial activity for choline and promotion for glycine synthesis in the host. This is reflected
444 by the depleted levels of faecal dimethylamine (DMA), trimethylamine (TMA), and elevated
445 concentrations of fecal choline and glycine as well as urinary choline and creatine. On one hand,
446 choline is usually derived from daily diet and can be metabolized into TMA via gut microbiota
447 and is further degraded to TMAO or DMA. On the other hand, host metabolises choline to
448 glycine via betaine, methionine and sarcosine, and then decomposes it into methylamine or
449 creatine, which is ultimately excreted as creatinine.⁴¹ Our result showed negative correlations
450 between DMA, TMA and band 10 and band 30, respectively; furthermore, band 10 was
451 negatively correlated to faecal methionine and sarcosine and positively associated with glycine
452 and creatinine. As previously reported,^{65,66} increased creatine and ethanolamine levels (data not
453 shown) in our study may maintain intestinal muscle contractions and osmoregulation. These
454 correlations suggest that *Enterobacter aerogenes* damaged normal functions of the gut. In
455 addition, *Enterobacter aerogenes* is able to produce putrescine and cadaverine⁶⁷ (which were
456 elevated in rats with diarrhea, data not shown), which are deemed to indulge histamine induced
457 diarrhea.^{68,69}

458 CF-induced diarrhea due to the intrusion of harmful bacteria and the suppression of helpful
459 microbial population, which is analogous to antibiotic treatments, can selectively sterilize normal
460 bacteria. It is different that the dysbiotic microflora in CF-treated rats returned to normal after 7
461 days of recovery (Figure S3), which does not occur in antibiotics treatments.^{17,65} Further
462 investigations should be performed to access the antimicrobial mechanism of CF because
463 antibiotics often promote the expression of antibiotic resistance genes in the microbiome.⁷⁰
464 Antibiotics not only cause dysbacteriosis but often down-regulate the levels of SCFAs, BCFAs,

465 methylamines, xanthine, uracil hippurate ect.⁴⁰ However, monosaccharides, BCAAs, aromatic
466 amino acids and choline were up-regulated in our CF-induced intestinal turbulence. What
467 amazed us is that the SCFA levels in urine showed an increasing trend which differed from
468 faeces. This distinction also found in antibiotics-treated metabolic profiles,⁴⁰ because faecal
469 metabolites primarily reflected the gut microbiota metabolism but urinary excretions usually
470 come from the host-microbiome co-metabolism. Metabolic perturbations related to changes in
471 physiological status are only present in urine. Thus, significant components in urine may not be
472 the direct metabolic products of gut microbiota but are altered along with other metabolites in
473 host's systemic circulation.

474 **Conclusion**

475 This work describes toxicity of CF in rats with diarrhea, and the variations in urinary and
476 faecal metabolites have been clarified by an NMR metabolomic study, while the expected
477 dysbiosis of gut microbiota were confirmed by DGGE analysis. Furthermore, we employed
478 covariation analyses of NMR and DGGE data to explore the impact of the altered gut microbial
479 on metabolic profiles of CF-treated rats. The findings indicate that excessive and long-term CF
480 administration perturbed some metabolic pathways such as glycine and serine degradation, and
481 then disturbed the harmonious growth of intestinal bacteria. In rats with diarrhea, *Bacteroides*
482 and *Prevotella* were significantly suppressed, while *Acidovorax*, *Enterobacter* and *Veillonella*
483 were promoted. The disrupted gut microflora may have caused the diarrhea in response to the
484 decreased SCFA levels, which play an irreplaceable role in regulating the absorption of water
485 and sodium. *Enterobacter* and *Veillonella* have indispensable roles in gut microbiota or host
486 metabolism due to their frequent and compact correlations with the alternations in energy
487 metabolism, amino metabolism and choline metabolism in faeces. *Bacteroides* and *Acidovorax*,

488 which are related to most of urinary metabolites such as BCAAs, hippurate, creatine and
489 glutamate, restructure host's metabolic phenotype after CF administration. According to this
490 study, we found that CF toxicity on gut is reversible using metabolic and DGGE trajectory chart.
491 In conclusion, this work inspired us to find a novel way to study drug toxicity. Moreover, global
492 system biology combined with metabonomics can yet be regarded as a commendable strategy for
493 TCM research.

494 **Abbreviations**

495 PCR-DGGE, polymerase chain reaction-denaturing gradient gel electrophoresis; BCFAs,
496 branched chain fatty acids; GC-MS, gas chromatography-mass spectrometry; LC-MS, liquid
497 chromatography-mass spectrometry; NMR, nuclear magnetic resonance; TSP, sodium 3-
498 (trimethylsilyl) propionate-2,2,3,3-*d*₄; HSQC, ¹H-¹³C heteronuclear single quantum correlation
499 spectroscopy; TCA, tricarboxylic acid cycle; VIP, variable importance to the projection.

500 **Acknowledgement**

501 This work was financially supported by the National Natural Science Foundation of China
502 (Grant No. 81173564, No. 81274028, No. 81473319 and No. 81473540), the National Key
503 Technology R&D Program during the Twelfth Five-Year Plan Period of People's Republic of
504 China (No. 2013BAD10B04-2) and the Guangzhou Science and Technology Program (No.
505 2014J4100176).

506 **Notes**

507 The authors declare no competing financial interest.

508

509 References

- 1 J. Tang, Y. Feng, S. Tsao, N. Wang, R. Curtain and Y. Wang, *J. Ethnopharmacol.* 2009, **126**, 5-17.
- 2 Z. Jiang, F. Liu, E. S. Ong and S. Li, *Metabolomics.* 2012, **8**, 1052-1068.
- 3 R. Shi, H. Zhou, B. Ma, Y. Ma, D. Wu, X. Wang, H. Luo and N. Cheng, *Biopharm. Drug Dispos.* 2012, **33**, 135-145.
- 4 X. Zhang, Y. Zhao, M. Zhang, X. Pang, J. Xu, C. Kang, M. Li, C. Zhang, Y. Zhang, X. Li, G. Ning and L. Zhao, *PloS One.* 2012, **7**.
- 5 Y. Zhou, Q. Liao, M. Lin, X. Deng, P. Zhang, M. Yao, L. Zhang and Z. Xie, *PLoS One.* 2014, **9**.
- 6 X. Zhao, X. Tong, L. Zhao, Q. Zhou, Z. Peng and B. Pang, *Zhongguo Zhong Yao Za Zhi.* 2013, **38**, 546-547.
- 7 M. G. Gareau and K. E. Barrett, *Curr. Opin. Pharmacol.* 2013, **13**, 895-899.
- 8 V. C. Antharam, E. C. Li, A. Ishmael, A. Sharma, V. Mai, K. H. Rand and G. P. Wang, *J. Clin. Microbiol.* 2013, **51**, 2884-2892.
- 9 J. M. Hollander and J. I. Mechanick, *J. Am. Diet. Assoc.* 2008, **108**, 495-509.
- 10 G. Xie, A. Zhao, L. Zhao, T. Chen, H. Chen, X. Qi, X. Zheng, Y. Ni, Y. Cheng, K. Lan, C. Yao, M. Qiu and W. Jia, *J. Proteome Res.* 2012, **11**, 3449-3457.
- 11 T. E. Cowan, M. S. Palmnäs, J. Yang, M. R. Bomhof, K. L. Ardell, R. A. Reimer, H. J. Vogel and J. Shearer, *J. Nutr. Biochem.* 2014, **25**, 489- 495.
- 12 W. Xie, D. Gu, J. Li, K. Cui and Y. Zhang, *PLoS One.* 2011, **6**.
- 13 J. Xia and D. S. Wishart, *Nucleic. Acids Res.* 2010, **38** (Suppl.), W71-77.
- 14 A. Subramanian, P. Tamayo, V. K. Mootha, S. Mukherjee, B. L. Ebert, M. A. Gillette, A.

- Paulovich, S. L. Pomeroy, T. R. Golub, E. S. Lander and J. P. Mesirov, *Proc. Natl. Acad. Sci. U.S.A.* 2005, **102**, 15545-15550.
- 15 C. Pontoizeau, J. F. Fearnside, V. Navratil, C. Domange, J. B. Cazier, C. Fernández-Santamaría, P. J. Kaisaki, L. Emsley, P. Toulhoat, M. T. Bihoreau, J. K. Nicholson, D. Gauguier and M. E. Dumas, *J. Proteome Res.* 2011, **10**, 1675-1689.
- 16 Y. Zhao, J. Wu, J. V. Li, N. Y. Zhou, H. Tang and Y. Wang, *J. Proteome Res.* 2013, **12**, 2987-2999.
- 17 J. R. Swann, K. M. Tuohy, P. Lindfors, D. T. Brown, G. R. Gibson, I. D. Wilson, J. Sidaway, J. K. Nicholson and E. Holmes, *J. Proteome Res.* 2011, **10**, 3590-3603.
- 18 J. Wu, Y. An, J. Yao, Y. Wang and H. Tang, *Analyst.* 2010, **135**, 1023-1030.
- 19 C. A. Merrifield, M. Lewis, S. P. Claus, O. P. Beckonert, M. E. Dumas, S. Duncker, S. Kochhar, S. Rezzi, J. C. Lindon, M. Bailey, E. Holmes and J. K. Nicholson, *Mol. BioSyst.* 2011, **7**, 2577-2588.
- 20 G. Le Gall, S. O. Noor, K. Ridgway, L. Scovell, C. Jamieson, I. T. Johnson, I. J. Colquhoun, E. K. Kemsley and A. Narbad, *J. Proteome Res.* 2011, **10**, 4208-4218.
- 21 M. E. Dumas, J. Kinross and J. K. Nicholson, *Gastroenterology.* 2014, **146**, 46-62.
- 22 M. Rantalainen, O. Cloarec, O. Beckonert, I. D. Wilson, D. Jackson, R. Tonge, R. Rowlinson, S. Rayner, J. Nickson, R. W. Wilkinson, J. D. Mills, J. Trygg, J. K. Nicholson and E. Holmes, *J. Proteome Res.* 2006, **5**, 2642-2655.
- 23 D. J. Crockford, E. Holmes, J. C. Lindon, R. S. Plumb, S. Zirah, S. J. Bruce, P. Rainville, C. L. Stumpf and J. K. Nicholson, *Anal. Chem.* 2006, **78**, 363-371.
- 24 S. Bastian Heymann and M. Jacomy, *International AAAI Conference on Weblogs and Social Media*; Association for the Advancement of Artificial Intelligence, CA, Palo

- Alto, 2009.
- 25 H. Lu, J. He, Z. Wu, W. Xu, H. Zhang, P. Ye, J. Yang, S. Zhen and L. Li, *Microb. Ecol.* 2013, **65**, 781-791.
- 26 X. Tan, J. Ma, R. Feng, C. Ma, W. Chen, Y. Sun, J. Fu, M. Huang, C. He, J. Shou, W. He, Y. Wang and J. Jiang, *PloS One.* 2014, **8**.
- 27 J. Ma, R. Feng, X. Tan, C. Ma, J. Shou, J. Fu, M. Huang, C. He, S. Chen, Z. Zhao, W. He, Y. Wang and J. Jiang, *J. Pharm. Sci.* 2013, **102**, 4181-4192.
- 28 X. Cha and C. Zhou, in *Biochemistry*, ed. N. Cheng, and A. Zhou, People's Medical Publishing House, Beijing, 2008, pp 179-206.
- 29 E. A. Smith and G. T. Macfarlane, *Anaerobe.* 1997, **3**, 327-337.
- 30 M. Blaut and T. Clavel, *J. Nutr.* 2007, **137** (Suppl. 2), 751-755.
- 31 J. K. Nicholson, E. Holmes and I. D. Wilson, *Nat. Rev. Microbiol.* 2005, **3**, 431-438.
- 32 S. E. Pryde, S. H. Duncan, G. L. Hold, C. S. Stewart, H. J. Flint, *FEMS Microbiol. Lett.* 2002, **217**, 133-139.
- 33 J. H. Cumming, J. L. Rombeau and T. Sakata, in *Physiological and clinical aspects of short-chain fatty acids*, ed. Cambridge University Press, Cambridge, 1995.
- 34 F. P. Martin, N. Sprenger, I. Montoliu, S. Rezzi, S. Kochhar, J. K. Nicholson, *J. Proteome Res.* 2010, **9**, 5284-5295.
- 35 Z. Wang, E. Klipfell, B. J. Bennett, R. Koeth, B. S. Levison, B. Dugar, A. E. Feldstein, E. B. Britt, X. Fu, Y. M. Chung, Y. Wu, P. Schauer, J. D. Smith, H. Allayee, W. H. Tang, J. A. DiDonato, A. J. Lusis, S. L. Hazen, *Nature.* 2011, **472**, 57-63.
- 36 X. Cha and C. Zhou, in *Biochemistry*, ed. Y. Wang, People's Medical Publishing House,

- Beijing, 2008, pp 120-159.
- 37 J. Xia and D. S. Wishart, *Nat. Protoc.* 2011, **6**, 743-760.
- 38 L. Stryer, J. M. Berg and T. L. Tymoczko, in *Biochemistry*, ed. W. H. Freeman and Company, New York, 2006.
- 39 X. Cha and C. Zhou, in *Biochemistry*, ed. X. Cui, People's Medical Publishing House, Beijing, 2008, pp 220-235.
- 40 X. Zheng, G. Xie, A. Zhao, L. Zhao, C. Yao, N. H. Chiu, Z. Zhou, Y. Bao, W. Jia, J. K. Nicholson and W. Jia, *J. Proteome Res.* 2011, **10**, 5512-5522.
- 41 S. S. Heinzmann, C. A. Merrifield, S. Rezzi, S. Kochhar, J. C. Lindon, E. Holmes and J. K. Nicholson, *J. Proteome Res.* 2012, **11**, 643-655.
- 42 F. Savino, L. Cordisco, V. Tarasco, E. Locatelli, D. Di Gioia, R. Oggero and D. Matteuzzi, *BMC Microbiology.* 2011, **11**, 157.
- 43 B. van den Bogert, M. Meijerink, E. G. Zoetendal, J. M. Wells and M. Kleerebezem, *PLoS One.* 2014, **9**.
- 44 H. Meng, Y. Zhang, L. Zhao, W. Zhao, C. He, C. F. Honaker, Z. Zhai, Z. Sun and P. B. Siegel, *PLoS One.* 2014, **9**.
- 45 F. H. Karlsson, D. W. Ussery, J. Nielsen and I. A Nookaew, *Microb. Ecol.* 2011, **61**, 473-485.
- 46 D. L. Topping and P. M. Clifton, *Physiol. Rev.* 2001, **81**, 1031-1064.
- 47 J. M. Wong, R. de Souza, C.W. Kendall, A. Emam and D. J. Jenkins, *J. Clin. Gastroenterol.* 2006, **40**, 235-243.
- 48 J. J. Kovarik, W. Tillinger, J. Hofer, M. A. Hözl, H. Heinzl, M. D. Saemann and G. J. Zlabinger, *Eur. J. Clin. Invest.* 2011, **41**, 291-298.

- 49 C. De Filippo, D. Cavalieri, M. Di Paola, M. Ramazzotti, J. B. Poullet, S. Massart, S. Collini, G. Pieraccini and P. Lionetti, *Proc. Natl. Acad. Sci. U.S.A.* 2010, **107**, 14691-14696.
- 50 B. A. White, R. Lamed, E. A. Bayer and H. J. Flint, *Annu. Rev. Microbiol.* 2014, **68**, 279-286.
- 51 H. Zhang, J. K. DiBaise, A. Zuccolo, D. Kudrna, M. Braidotti, Y. Yu, P. Parameswaran, M. D. Crowell, R. Wing, B. E. Rittmann and R. Krajmalnik-Brown, *Proc. Natl. Acad. Sci. U.S.A.* 2009, **106**, 2365-2370.
- 52 F. Brito, C. Zaltman, A. T. Carvalho, R. G. Fischer, R. Persson, A. Gustafsson and C. M. Figueredo, *Eur. J. Gastroenterol. Hepatol.* 2013, **25**, 239-245.
- 53 G. D. Wu, F. D. Bushman and J. D. Lewis, *Anaerobe*. 2013, **24**, 117-120.
- 54 M. Pop, A. W. Walker, J. Paulson, B. Lindsay, M. Antonio, M. A. Hossain, J. Oundo, B. Tamboura, V. Mai, I. Astrovskaya, H. Corrada Bravo, R. Rance, M. Stares, M. M. Levine, S. Panchalingam, K. Kotloff, U. N. Ikumapayi, C. Ebruke, M. Adeyemi, D. Ahmed, F. Ahmed, M. T. Alam, R. Amin, S. Siddiqui, J. B. Ochieng, E. Ouma, J. Juma, E. Mailu, R. Omere, J. G. Morris, R. F. Breiman, D. Saha, J. Parkhill, J. P. Nataro and O. C. Stine, *Genome. Biol.* 2014, **15**, R76.
- 55 O. Revelles, M. Espinosa-Urgel, T. Fuhrer, U. Sauer and J. L. Ramos, *J. Bacteriol.* 2005, **187**, 7500-7510.
- 56 A. P. Corfield, S. A. Wagner, J. R. Clamp, M. S. Kriaris, and L. C. Hoskins, *Infect. Immun.* 1992, **60**, 3971-3978.
- 57 J. C. Byrd and R. S. Bresalier, *Cancer Metast. Rev.* 2004, **23**, 77-99.
- 58 D. Monleon, J. M. Morales, A. Barrasa, J. A. López, C. Vázquez and B. Celda, *NMR*

- Biomed.* 2009, **22**, 342-348.
- 59 S. Kang, S. E. Denman, M. Morrison, Z. Yu, J. Dore, M. Leclerc and C. S. McSweeney, *Inflamm. Bowel. Dis.* 2010, **16**, 2034-2042.
- 60 S. O. Noor, K. Ridgway, L. Scovell, E. K. Kemsley, E. K. Lund, C. Jamieson, I. T. Johnson and A. Narbad, *BMC Gastroenterol.* 2010, **12**, 134.
- 61 B. Samb-Ba, C. Mazonot, A. Gassama-Sow, G. Dubourg, H. Richet, P. Hugon, J. C. Lagier, D. Raoult and F. Fenollar, *PLoS One.* 2014, **9**.
- 62 R. Cermak and G. M. Breves, *Arch. Anim. Nut.* 2006, **60**, 180-189.
- 63 J. K. Nicholson, E. Holmes, J. Kinross, R. Burcelin, G. Gibson, W. Jia and S. Pettersson, *Science.* 2012, **336**, 1262-1267.
- 64 T. A. Clayton, *FEBS Lett.* 2012, **586**, 956-961.
- 65 F.P. Martin, Y. Wang, I.K. Yap N. Sprenger, J. C. Lindon, S. Rezzi, S. Kochhar, E. Holmes and J. K. Nicholson, *J. Proteome Res.* 2009, **8**, 3464-3474.
- 66 P. H. Yancey, M. E. Clark, S. C. Hand, R. D. Bowlus and G. N. Somero, *Science.* 1982, **217**, 1214-1222.
- 67 P. Kalač, *Meat Sci.* 2006, **73**, 1-11.
- 68 H. P. Til, H. E. Falke, M. K. Prinsen and M. I. Willems, *Food Chem. Toxicol.* 1997, **35**, 337-348.
- 69 S. Bodmer, C. Imark and M. Kneubühl, *Inflamm. Res.* 1999, **48**, 296-300.
- 70 S. R. Modi, J. J. Collins and D. A. Relman, *J. Clin. Invest.* 2014, **124**, 4212-4218.

Supporting Information

Figure S1 shows 600 MHz ^1H NMR spectra of **faeces** and urine of SD rat, **Figure S2** shows PCA scores scatter plots for ^1H NMR data of urine and **faeces**, **Figure S3** shows PCA scores scatter plot for DGGE fingerprint of day 21. **Table S1** and **S2** list specific assignments of faecal and urinary metabolites. **Table S3** and **S4** exhibit results about quantitative enrichment analysis and pathway analysis of **faecal** metabolites on day 7. **Table S5** and **S6** exhibit similar results like Table S3 and S4 about urine.

Figure legends

Figure 1 ^1H NMR coefficient loading profiles from OPLS-DA model on day 7 and PLS-DA scores plots with time-dependent trajectory. A is for urine samples, B is for faeces and in C graph: (1), (2), (3) exhibit fluctuations of 4, 3, 3 time points in urine, faeces and microbiota respectively.

Figure 2 Distributions of intensities for selected urinary metabolites based upon the normalized bucket table. Significant metabolites of rats' urine which compared control group with CF-treated group at different time points: day -1 is pre-administration day, day 7 and day 14 are diarrhea days, and day 21 is post-administration day for 7 days.

Figure 3 Distributions of intensities for selected faecal metabolites based upon the normalized bucket table. **Significant metabolites of faeces samples from CF-treated group were compared with control group ones at different time points: day -1 is pre-administration day, day 7 is diarrhea at the first day.**

Figure 4 Meaningful metabolic pathways of urine and faeces from MSEA. 57 components in faeces were imported to MSEA to show really changed pathways (A-1), a weight distribution of these pathways displayed on the right hand (A-2). 85 urinary metabolites were conducted as faecal samples, and results exhibited in B-1, B-2 severally. At the right corner of each block scheme, it emerged the specific pathway which detected metabolites were involved in (rectangles colored in blue are no metabolites matched, vice versa).

Figure 5 16S rDNA PCR-DGGE on day 7, the red marked bands are significant in diarrhea progressing. OPLS-DA coefficient loading profile (right) displayed the discriminative DGGE bands by comparing the treated group with control.

Figure 6 Correlation network between altered DGGE bands (the corresponding bacterial species in Table 1) and changed metabolic components of rats' urine and faeces visualized with Gephi. This map calculated using Pearson correlation coefficients ($|r| \geq 0.755$ and $p < 0.05$), and node size denotes the highest effect size for each band or metabolite comparing treated group with control group. Nodes colored red for bands, amaranth for faecal metabolites and cyan for urinary ones. Red lines correspond to positive correlations, whereas blue lines correspond to negative correlations.

Table 1 Closest relatives of 16S rDNA V3 regions sequences derived from DGGE bands.